

## A new plasmopause location model based on THEMIS observations

LIU Xu<sup>1,2</sup> & LIU WenLong<sup>1\*</sup>

<sup>1</sup>Space Science Institute, School of Astronautics, Beihang University, Beijing 100191, China;

<sup>2</sup>State Key Laboratory of Space Weather, Chinese Academy of Sciences, Beijing 100190, China

Received September 4, 2013; accepted February 10, 2014; published online May 28, 2014

A new empirical model of plasmopause location as functions of magnetic local time and geomagnetic indices has been developed based on the observations from THEMIS mission. We use the two-year data of electron density inferred from spacecraft potential to identify the plasmopause crossings and create a database of plasmopause locations. The database is further used to build up an empirical model of plasmopause related to magnetic local time based on the equation from O'Brien and Moldwin (2003). The new model is compared with previous plasmopause location models. It is found that our newly developed model is the best in predicting plasmopause locations among the existing models. The models based on Kp and Dst indices are better than the model based on AE index, suggesting that the plasmopause location is controlled by large scale convection of the magnetosphere.

**plasmopause, geomagnetic index, magnetic local time**

**Citation:** Liu X, Liu W L. 2014. A new plasmopause location model based on THEMIS observations. *Science China: Earth Sciences*, 57: 2552–2557, doi: 10.1007/s11430-014-4844-1

The plasmasphere is an important component of the inner magnetosphere, filled with low-energy particles, which are indentured by the large-scale electric field and co-rotate with the Earth. The outer boundary of the plasmasphere is called 'plasmopause'. Because of the differences of plasma properties across the boundary, plasmopause plays important roles in controlling the distribution of the inner magnetospheric particles (Lorentzen et al., 2001), influencing the formation and propagation of electromagnetic waves (Orr and Webb, 1975; Webb and Orr, 1975; Takahashi and Anderson, 1992; Liu et al., 2009, 2011, 2013), and subsequently affecting the ring current (Kozyra et al., 1995; Lorentzen et al., 2001) and radiation belt (Horne and Thorne, 1998; Lorentzen et al., 2001; Li et al., 2006). Thus, plasmopause location ( $L_{pp}$ ) is considered as a crucial parameter

in the research of inner magnetosphere dynamic. Plasmopause location is determined by the balance between large-scale co-rotation electric field and convective electric field influenced by geomagnetic activities. For example, during magnetic active periods, the plasmasphere is compressed due to the enhancement of large-scale convective electric field, whereas during magnetic quiet periods, the plasmasphere expands gradually (Carpenter and Anderson, 1992). Besides its radial movement, the plasmopause can have complicated structures, such as plume, shoulder, notch, and channel (Zhang et al., 2013).

Based on in situ observations, several empirical models have been established for the estimation of  $L_{pp}$ . For example, the model proposed by Carpenter and Anderson (1992) considered  $L_{pp}$  as a linear function of Kp index. Because of the lack of satellite measurements (208 plasmopause crossings by ISEE satellite), their research only covered the sec-

\*Corresponding author (email: liuwenlong@buaa.edu.cn)

tor of 00:00–15:00 magnetic local time (MLT). A linear equation was suggested to describe the relation between  $L_{pp}$  and the maximum Kp index in the time period from the previous 24 hours to the previous 4 hours,

$$\hat{L}_{pp} = 5.6 - 0.46 \times \max_{-24, -4} Kp. \quad (1)$$

Based on the 969 identified plasmopause crossings, Moldwin et al. (2002) found relationships between  $L_{pp}$  and the maximum Kp index during the previous 12 hours for nightside, dawnside, dayside, and duskside, respectively,

$$\hat{L}_{pp} = A + B \times \max_{-12, 0} Kp, \quad (2)$$

where  $A$  and  $B$  were two fitted parameters.

Given that the plasmopause is not only a linear function of Kp index but also linear functions of AE and Dst indices, the model proposed by O'Brien and Moldwin (2003) compared the differences among the three geomagnetic indices. The model is described as

$$\hat{L}_{pp} = a + b \times \text{INDEX}, \quad (3)$$

where INDEX stands for the logarithm of maximum AE index during the previous 36 hours ( $\log_{10} \max_{-36, 0} \text{AE}$ ), the logarithm of absolute value of minimal Dst index during the previous 24 hours ( $\log_{10} |\min_{-24, 0} \text{Dst}|$ ), or maximum Kp index during the time period from previous the 36 hours to the previous 2 hours ( $\log_{10} \max_{-36, -2} Kp$ ).

O'Brien and Moldwin (2003) also established an  $L_{pp}$  model for MLT and geomagnetic indices based on the following formula.

$$\begin{cases} \phi = 2\pi(\text{MLT}/24), \\ L_{pp} = a_1 \left[ 1 + a_{\text{MLT}} \cos(\phi - 2\pi a_\phi / 24) \right] \text{INDEX} \\ \quad + b_1 \left( 1 + b_{\text{MLT}} \cos(\phi - 2\pi b_\phi / 24) \right). \end{cases} \quad (4)$$

This model could describe more details of the plasmopause for different magnetic local time.

The current plasmopause models cannot cover the whole inner magnetosphere. For example, the plasmopause crossing data used for establishing Carpenter and Anderson (1992) model are limited in the MLT sector between 00:00 and 15:00; the other two models used observations of few crossing at the dayside high altitude region because of the orbit of CRRES satellite. Moreover, the first three empirical models do not contain MLT information, and the fourth MLT model has less prediction accuracy (O'Brien and Moldwin, 2003). Thus, it is necessary to establish a new model of plasmopause location as functions of MLT and geomagnetic indices. In this paper, using the observations from THEMIS-D satellite from 2011 to 2012, we establish a database of plasmopause crossings. After analyzing the property and distribution of plasmopause location, we establish a plasmopause model related to MLT and geomagnetic indices. We then compare our model with the four

previous models mentioned above.

## 1 THEMIS observation of plasmopause crossings

### 1.1 The identification of plasmopause crossing

The data used in this paper are obtained by the NASA's THEMIS mission. The five THEMIS satellites were launched on February 17, 2007, aiming to study substorm, storm, and other space physical phenomena. The orbit of THEMIS-D satellite is with an apogee of  $\sim 12R_E$ , a perigee of  $\sim 1.5R_E$ , and an inclination of  $9^\circ$ . The satellite passes through the plasmopause twice in each orbit period and finishes a full coverage of all local time sectors of the inner magnetosphere once per year.

In this paper, we study the electron density derived from the satellite potential observed by THEMIS-D in 2010 and 2011. The electron density referred by this method has an error of a factor of 2 (Pedersen et al., 1998), which is much smaller than a typical density change across a plasmopause and thus is sufficient for the identification of plasmopause location (Li et al., 2010). Here we use the criteria suggested by Carpenter and Anderson (1992) and used by other studies (e.g., Moldwin et al., 2002; O'Brien and Moldwin, 2003) for identifying plasmopause location, which requires plasma density changes by a factor of 5 within  $0.5L$ . We first mark the position where plasma density changes more than a factor of 5 within  $0.5L$  around this position, and then consider the region constituted by the marked position is the plasmopause region. The center position of this region is defined as plasmopause location and the width of this region is defined as the width of the plasmopause.

Figure 1 illustrates an example of electron density measurements observed on February 2, 2010 by THEMIS-D satellite. THEMIS-D observes two electron density gradients at 01:20 and 21:20UT, respectively. The variations of both electron density gradients are about 3 orders and satisfy the plasmopause criteria. Thus we find two plasmopause crossings, which correspond to the inbound and outbound orbit, respectively. The rectangles in Figure 1 mark the plasmopause regions. The center positions of the rectangles are the plasmopause locations where  $L$  value equals to 4.97 and 4.94, and their width are  $0.46R_E$  and  $0.52R_E$ , respectively.

Data in 2010 and 2011 are analyzed using the same method, from which 1427 plasmopause crossing events are identified. The electron density profile of plasmopause shown in Figure 1 is 'classic' plasmopause with one sharp density variation. However, the change of electron density at plasmopause can be very complicated, either with gradually varying electron density or with multiple density gradients. Among the 1427 plasmopause crossing events, we observed 121 gradually varying plasmopause, 1183 plasmopause with one sharp gradient, and 123 plasmopause with multiple density gradients.

In the rest of this paper, we study the 'classic' plasmopause

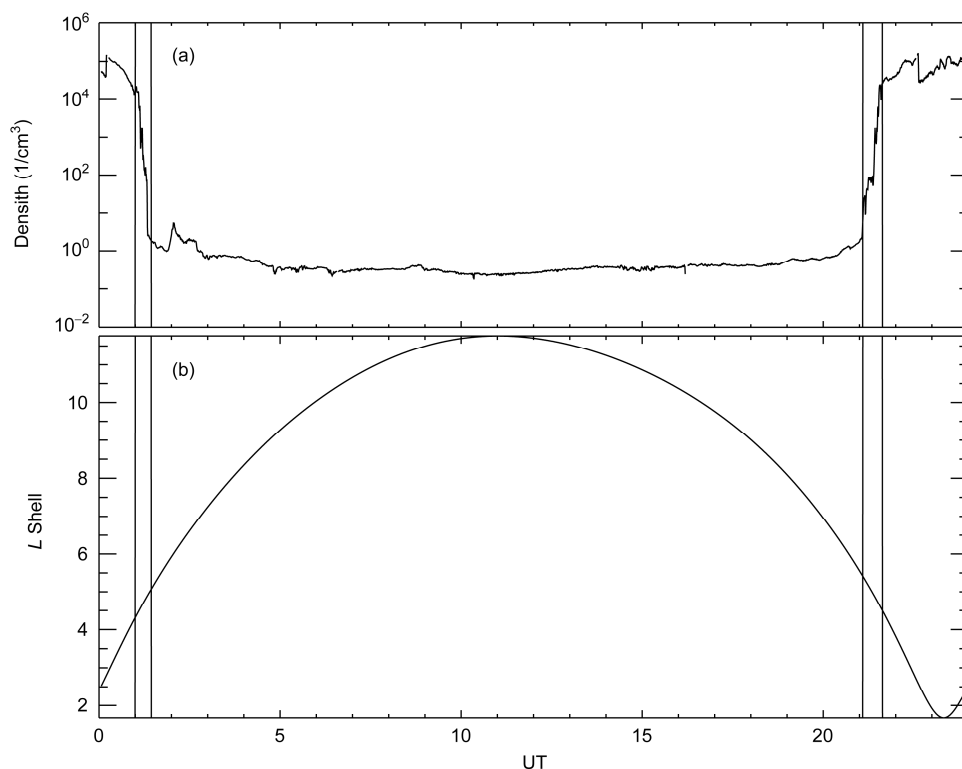


**Figure 1** Time series of electron density in the top panel and  $L$  shell in the bottom panel observed on February 2, 2010 by THEMIS-D satellite. The rectangles mark the two plasmapause regions.

with one sharp electron density gradient, which is consistent with the four models of plasmapause mentioned in the introduction session. The other types of plasmapause will be studied in the future.

## 1.2 The distribution of the plasmapause location

We plot the distribution of positions of the observed 1183 plasmapause versus LT in Figure 2(a). The plasmapause is located mostly in the region between  $L=3$  and  $L=6$ , and is distributed evenly in different LT sectors, with 346 in the nightside (21:00–03:00LT), 251 in the dawnside (03:00–09:00LT), 291 in the dayside (09:00–15:00LT), and 295 in the duskside (15:00–21:00LT), respectively. Figure 2(b) shows the statistic distribution of the width of plasmapause, which is mostly between  $0.2 R_E$  and  $0.6 R_E$  and could be as wide as  $2 R_E$ .

## 2 New MLT dependent plasmapause location model

### 2.1 Geomagnetic indices

The geomagnetic indices (Dst, AE, Kp) used to establish our model are obtained from the World Data Center for Geomagnetism of Kyoto University (<http://wdc.kugi.kyoto-u.ac.jp>).

### 2.2 Fitting for parameters

We use the same formula with O'Brien and Moldwin (2003) MLT model to fit our THEMIS plasmapause crossing database and build our MLT dependent plasmapause location model. The model is as follows,

$$\begin{aligned} \phi &= 2\pi(\text{MLT}/24), \\ \hat{L}_{pp} &= a_1 \left[ 1 + a_{\text{MLT}} \cos(\phi - 2\pi a_\phi / 24) \right] \times \text{INDEX} \\ &\quad + b_1 \left[ 1 + b_{\text{MLT}} \cos(\phi - 2\pi b_\phi / 24) \right], \end{aligned} \quad (5)$$

where INDEX stands for the logarithm of maximum AE index during the previous 36 hours ( $\log_{10} \max_{-36,0} \text{AE}$ ), the logarithm of absolute value of minimal Dst index during the previous 24 h ( $\log_{10} |\min_{-24,0} \text{Dst}|$ ), or maximum Kp index during the time period from the previous 36 hours to the previous 2 h ( $\log_{10} \max_{-36,-2} \text{Kp}$ ). The parameters obtained by fitting our observation database are shown in Table 1, for AE, Dst, and Kp indices, respectively.

### 2.3 Comparison between new model and previous models

This new MLT model of plasmapause could describe the position of plasmapause more precisely. Table 2 shows the prediction errors of the different models (the deviation between the  $L$  Shell value predicted by the model and the

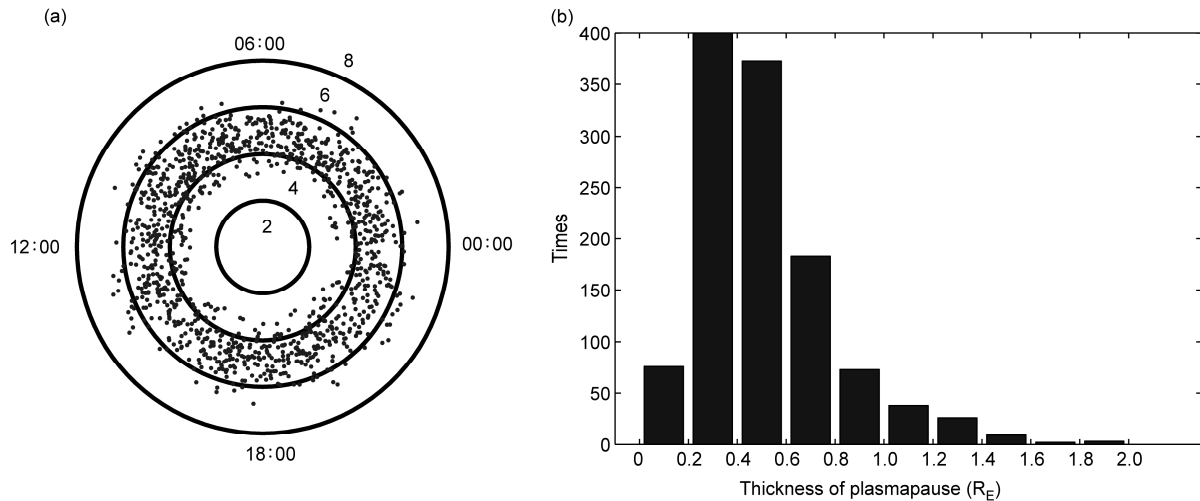


**Figure 2** The distribution of plasmopause for different local time (a) and histogram of the width of plasmopause (b).

**Table 1** The parameters of the magnetic local time model of plasmopause based on THEMIS observation

Indices	Parameters					
	$a_1$	$a_{MLT}$	$a_\phi$	$b_1$	$b_{MLT}$	$b_\phi$
AE	-1.254	-0.218	18.52	8.199	0.0757	6.91
Dst	-1.111	-0.2416	21.502	6.03	-0.0565	23.3214
Kp	-0.338	-0.286	21.045	5.729	-0.0428	23.0397

observed data by THEMIS) on July 2, 2011. The three rows correspond to Kp, Dst, and AE indices, respectively. The prediction errors of THEMIS Kp, Dst, and AE indices are  $0.0004R_E$ ,  $0.0175R_E$ , and  $0.1663R_E$ , which are less than that in other models.

Figure 3 shows the observation and the fitting curve of plasmopause for geomagnetic indices respectively. The Dst and Kp models could fit the THEMIS database well in 00:00–18:00 MLT sectors. However, during 18:00–24:00 MLT, the errors are relatively larger compared with other sectors because of the dynamic processes in the duskside and nightside.

In order to quantitatively compare the THEMIS model with previous models, we calculate the RMSE (Root Mean Square Error) value for each model using the observed data  $L_{pp}$  and the prediction value  $\hat{L}_{pp}$  by the different model, as defined by

$$RMSE = \sqrt{\left( \sum_{i=1}^n (L_{ppi} - \hat{L}_{ppi})^2 \right) / n}, \quad (6)$$

where the less the RMSE value is, the more precise the model is.

Table 3 shows the RMSE value of our THEMIS MLT model, Moldwin et al. (2002) model, O'Brien and Moldwin (2003) model, O'Brien and Moldwin (2003) MLT model, and Carpenter and Anderson (1992) model. From this table, we can see that, in general, the Dst and Kp models can better predict the plasmopause location than the AE model, which is probably because the plasmopause is controlled by the large-scale convection in the magnetosphere.

By comparing the models in Figure 3, we find the RMSE values of THEMIS models are 0.6319, 0.6040, and 0.6094 for AE, Dst, and Kp models respectively, which are smaller than the RMSE values of previous models. Moreover, the RMSE values of Dst and Kp model are large in the duskside and nightside, which is consistent with Figure 3.

The O'Brien and Moldwin (2003) Dst and Kp model also can do a good job in term of predicting the plasmopause locations of our database with RMSE values of 0.6835 and 0.6401, which are slightly higher than our model. The Carpenter and Anderson (1992) model gets an RMSE value of 0.6977, which means this model could basically describe the THEMIS database. Moldwin et al. (2002) model has a large RMSE value, especially in dayside and duskside with RMSE values of 0.9193 and 1.0211 respectively, suggesting

**Table 2** The comparison of prediction errors of different plasmopause models on July 2, 2011 (unit:  $R_E$ )

	THEMIS model	O'Brien and Moldwin (2003) model	O'Brien and Moldwin (2003) MLT model	Moldwin et al. (2002) model	Carpenter and Anderson (1992) model
AE	0.1663	0.7540	0.4574		
Dst	0.0175	0.2935	0.1506		
Kp	0.0004	0.1176	0.0156	0.4668	0.2534

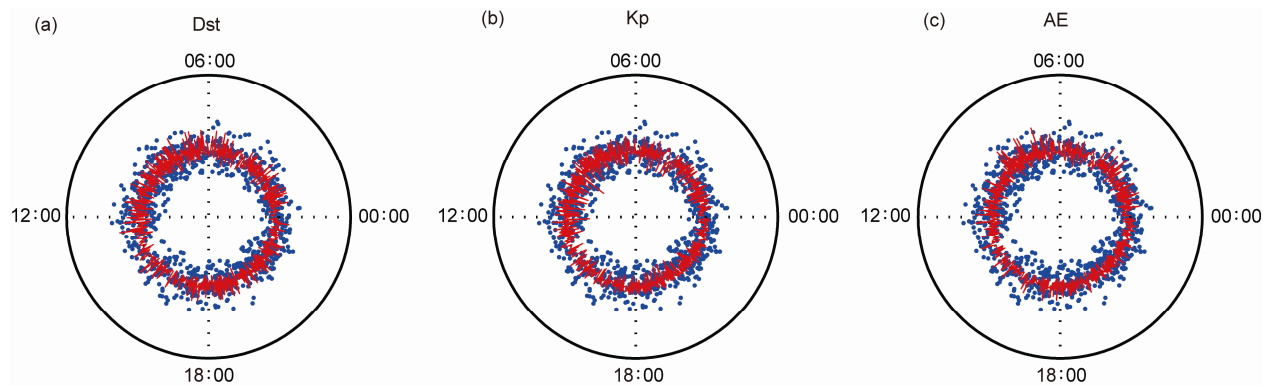


**Figure 3** The relationship between plasmopause position and THEMIS magnetic local time model: (a)  $\max_{-24,0}$ Dst model, containing data of all local time; (b)  $\max_{-36,-2}$ Kp model, containing data of all local time; (c)  $\max_{-36,0}$ AE model, containing data of all local time. The blue points stand for the observed data by THMMIS, and red lines stand for the fitting curves.

**Table 3** The RMSE value of THEMIS model and current model

Model	Geomagnetic indices	Magnetic local time sector				
		00:00–24:00	21:00–03:00	03:00–09:00	09:00–15:00	15:00–21:00
THEMIS model	AE	0.6319	0.5647	0.6358	0.6635	0.6642
	Dst	0.6040	0.5438	0.6142	0.6358	0.6237
	Kp	0.6094	0.5557	0.6228	0.6129	0.6422
Moldwin et al. (2002) model	Kp	0.7139	0.6529	0.7295	0.9193	1.0211
O’Brien and Moldwin (2003) model	AE	0.8107	0.7340	0.7693	0.8222	0.9068
	Dst	0.6835	0.6175	0.6313	0.7416	0.7451
	Kp	0.6401	0.5838	0.6254	0.6454	0.6998
O’Brien and Moldwin (2003) MLT model	AE	0.8661	0.7488	0.8335	1.0924	0.8085
	Dst	0.7380	0.5762	0.7242	0.9323	0.7215
	Kp	0.7435	0.5875	0.6468	0.9313	0.8055
Carpenter and Anderson (1992) model	Kp	0.6977 (00:00–15:00MLT)				

this model cannot well predict the observations by THEMIS.

Table 3 also shows results of the O’Brien and Moldwin (2003) MLT model. We can see that this model has the largest RMSE values among all the models, suggesting that it could be greatly improved with our model.

### 3 Discussion and conclusion

Using the plasmopause crossing database created based on the THEMIS-D satellite, we have established an MLT dependent empirical model for plasmopause location, and then compared it with four previous models. We find that our new model can best predict the database, especially for Dst and Kp model suggesting that storm-time large-scale convection is the main factor controlling the position of the plasmopause. In fact, besides controlling the plasmopause position, the large-scale convective electric field controls the position of inner boundary of plasma sheet (Ding et al., 2010; Cao et al., 2011; Wang and Zong, 2012; Fu et al.,

2010a, 2010b).

The Carpenter and Anderson (1992) model was established based on the ISEE observation in 1977, 1982, and 1983. The other three models were established based on CRRES observation in 1990 and 1991, only containing the information during solar maximum year. The database in this paper is created based on the THEMIS observation in 2010 and 2011, containing more data and corresponding to the ascending phase of solar activities. In different phases of solar activities, different solar wind properties affect Earth’s magnetosphere: during the solar maximum period, enhanced CME events can trigger strong magnetic storms; during the ascending phase, the storms are driven mainly by co-rotating interaction region and thus are relatively weak. Thus in different phase of solar cycle, the plasmopause, controlled by large-scale convective electric field, responses differently on solar wind conditions. This could partially explain the difference between our model and previous models.

Moreover, extreme magnetic storm events, such as the super storm on March 24, 1991, can introduce errors into

previous models. However, our database is created during the ascending phase of solar activities and there is no strong geomagnetic activity, which makes our model less affected by super storms. This is probably a reason that, although using the same formulae with O'Brien and Moldwin (2003) MLT model, our model gets a better prediction (see in Table 3).

At last, our database is based on only two years' data. To get completed information about the plasmapause location, we still need a larger amount of data that could cover the whole solar cycle. This work reminds us of the necessity of improving the plasmapause models by analyzing more satellite data, filling our plasmapause database and hopefully building a more precise plasmapause model based on the satellite observation in the future.

*This work is supported by the National Natural Science Foundation of China (Grant Nos. 41104109, 41274166) and the Specialized Research Fund for State Space Weather Key Laboratories (Grant No. 201203FSK05). We acknowledge the THEMIS satellite data center and Kyoto University for providing the satellite data and geomagnetic indices data respectively. And we also acknowledge the valuable discussions with Dr. Jinbin Cao, Huishan Fu, Liuyuan Li, and Yudian Ma.*

- Cao J B, Ding W Z, Reme H, et al. 2011. The statistical studies of the inner boundary of plasma sheet, *Ann Geophys*, 29: 289–298, doi: 10.5194/angeo-29-289-2011
- Carpenter D L, Anderson R R. 1992. An ISEE/whistler model of equatorial electron density in the magnetosphere, *J Geophys Res*, 97: 1097–1108
- Ding W Z, Cao J B, Zeng L, et al. 2010. Simulation studies of plasma sheet ion boundary (in Chinese). *Chin J Geophys*, 53: 1505–1514
- Fu H S, Tu J, Cao J B, et al. 2010a. IMAGE and DMSP observations of a density trough inside the plasmasphere. *J Geophys Res*, 115: A07227, doi: 10.1029/2009JA015104
- Fu H S, Tu J, Song P, et al. 2010b. The nightside-to-dayside evolution of the inner magnetosphere: Imager for Magnetopause-to-Aurora Global Exploration Radio Plasma Imager observations. *J Geophys Res*, 115: A04213, doi: 10.1029/2009JA014668
- Horne R B, Thorne R M. 1998. Potential waves for relativistic electron scattering and stochastic acceleration during magnetic storms. *Geophys Res Lett*, 25: 3011–3014
- Kozyra J U, Rasmussen C E, Miller R H et al. 1995. Interaction of ring current and radiation belt protons with ducted plasmaspheric hiss, 2. Time evolution and distribution function. *J Geophys Res*, 100: 21911–21919
- Li X, Baker D N, O'Brien, et al. 2006. Correlation between the inner edge of outer radiation belt electrons and the inner most plasmapause location. *Geophys Res Lett*, 33: L14107, doi: 10.1029/2006GL026294
- Li W, Thorne R M, Bortnik J, et al. 2010. Global distributions of super-thermal electrons observed on THEMIS and potential mechanisms for access into the plasmasphere. *J Geophys Res*, 115: A00J10, doi: 10.1029/2010JA015687
- Liu W L, Cao J B, Li X, et al. 2013. Poloidal ULF wave observed in the plasmasphere boundary layer. *J Geophys Res-Space Physics*, 118: 4298–4307, doi: 10.1002/jgra.50427
- Liu W L, Sarris T E, Li X, et al. 2009. Electric and magnetic field observations of Pc4 and Pc5 pulsations in the inner magnetosphere: A statistical study. *J Geophys Res*, 114: A12206, doi: 10.1029/2009JA014243
- Liu W L, Sarris T E, Li X, et al. 2011. Spatial structure and temporal evolution of a dayside poloidal ULF wave event. *Geophys Res Lett*, 38: L19104, doi: 10.1029/2011GL049476
- Lorentzen K R, Blake J B, Inan U S, et al. 2001. Observations of relativistic electron microbursts in association with VLF chorus. *J Geophys Res*, 106: 6017–6027
- Moldwin M B, Downward L, Rassoul H K, et al. 2002. A new model of the location of the plasmapause: CRRES results. *J Geophys Res*, 107: 1339, doi: 10.1029/2001JA009211
- O'Brien T P, Moldwin M B. 2003. Empirical plasmapause models from magnetic indices. *Geophys Res Lett*, 30: 1152, doi: 10.1029/2002GL-016007
- Orr D, Webb D. 1975. Statistical studies of geomagnetic pulsations with periods between 20 and 120 sec and their relationship to the plasmapause region. *Planet Space Sci*, 23: 1169
- Pedersen A, Mozer F, Gustafsson G. 1998. Electric field measurements in a tenuous plasma with spherical double probes, in *Measurement Techniques in Space Plasmas: Fields*. *Ann Geophys-Geophys Monogr Ser*, 103: 1–12
- Takahashi K, Anderson B J. 1992. Distribution of ULF energy ( $f < 80$  mHz) in the inner magnetosphere: A statistical analysis of AMPTE CCE magnetic field data. *J Geophys Res*, 97: 10751–10773
- Wang Y F, Zong Q G. 2012. Study of the nose event on 11 April 2002 with UBK method. *Sci China Tech Sci*, 55: 1929–1942, doi: 10.1007/s11431-012-4862-1
- Webb D, Orr D. 1975. Spectral studies of geomagnetic pulsations with periods between 20 and 120 sec and their relationship to the plasmapause region. *Planet Space Sci*, 23: 1551–1561
- Zhang H, Xue R L, Shen C, et al. 2013. The simulation of the plasmapause structure during geomagnetic turbulence (in Chinese). *Chin J Geophys*, 56: 731–737, doi: 10.6038/cjg20130302